Observations of Parametric Fluorescence and Oscillation in the Infrared

James E. Pearson, Amnon Yariv, and Uri Ganiel

Measurements of infrared optical parametric fluorescence are reported for the first time. Using a pump wavelength of 1.064 μ in $LiNbO_3$, observations of the fluorescence power, bandwidth, and angular dependence at 1.63 μ are in good agreement with a plane-wave theory. The operating characteristics of two pulsed, internal, doubly resonant parametric oscillators are also reported and compared with predictions of the fluorescence measurements. With measured thresholds on the order of 400–700 W, the two oscillators provided nearly continuous tuning from 1.51 μ to 3.55 μ with average powers of 6 mW and peak powers of 600 W. These powers represent available pump conversion efficiencies of 10% and 50%, respectively. Oscillating bandwidths were only 10% of the fluorescence bandwidth and ranged from 1.7 cm^{-1} to 45 cm^{-1}, depending on the output wavelength. Longitudinal mode structure and multiple pulsing of the oscillators were observed.

I. Introduction

The recent advent of tunable coherent sources has greatly increased the potential usefulness of laser-related devices. Because of its versatility and wide tuning range, the optical parametric oscillator (OPO) is emerging as one of the most important sources of tunable coherent radiation, particularly in the infrared portion of the spectrum. With a few exceptions,[1-5] most reported OPO systems have used pumping lasers emitting in the visible.[6-11] The reports on infrared-pumped oscillators have not given detailed operating characteristics, and there have been no infrared measurements of parametric fluorescence, the basic process that drives an OPO.

This paper attempts to fill some of the gaps in the current literature on infrared-pumped OPO systems. We report for the first time detailed measurements of infrared parametric fluorescence using a technique that should be applicable to other potential infrared OPO systems. Parametric fluorescence data are very useful in evaluating a potential laser–nonlinear crystal OPO system since the crystal nonlinear coefficient[12] as well as the OPO tuning curve[5,13-15] and expected bandwidth[12] can be measured before the OPO is constructed.

Following a discussion of the fluorescence results, we present detailed observations on the properties of two 1.06-μ-pumped, doubly resonant, pulsed, $LiNbO_3$ parametric oscillators. The oscillators use the internal configuration, where the OPO is placed inside the pump laser resonator. The observed threshold and bandwidth of the two oscillators exhibit only approximate agreement with theory, although the tuning characteristics are accurately predicted. In terms of the available 1.06-μ power, reasonable average power conversion efficiencies ($\simeq$10%) and good peak power conversion efficiencies ($\simeq$50%) are observed. The multiple pulsing that is characteristic of internal, pulsed OPO systems[16] is observed, and the first observation of OPO longitudinal mode structure is reported.

The authors are with the California Institute of Technology, Pasadena, California 91109.

Received 6 December 1972.

II. Parametric Fluorescence

A. Theory

Parametric fluorescence was first discussed in 1961 by Louisell et al.[17] Since that time, comprehensive theoretical treatments have appeared[12,18,19] along with numerous experimental observations.[12-15,20] For later comparison with experimental observations, we review here some of the theoretical properties of parametric fluorescence. The following discussion follows the plane-wave analysis of Byer and Harris.[12]

The signal fluorescence power at ω_1, within $d\omega_1$, and emitted in the small solid angle $2\pi\phi\, d\phi$ is given by

$$dP_1 = K\omega_1^4\omega_2 l^2 P_3\, \mathrm{sinc}^2(\Delta kl/2)\phi\, d\phi\, d\omega_1, \qquad (1)$$

where $\mathrm{sinc}(x) = \sin(x)/x$, P_3 is the pump power, and K is a constant given by Byer and Harris.[12] By using a Taylor series expansion about the collinear phase-matched frequencies, the phase mismatch can be written for small angles as

$$\Delta k = -b_0\omega - b_1\omega^2 + G\phi^2, \quad (2)$$

where ϕ is the angle between the pump and signal wave vectors. The frequency in Eq. (2) is defined as the deviation from the collinear phase-matched frequencies ($\omega \equiv \omega_1 - \omega_{10} = \omega_{20} - \omega_2$). The expansion coefficients in Eq. (2) are thus

$$G = (k_{10}k_3)/2k_{20}, \quad (3)$$

$$b_0 = (\partial k_1/\partial\omega_1)_{\omega_{10}} - (\partial k_2/\partial\omega_2)_{\omega_{20}}, \quad (4)$$

$$b_1 = \frac{1}{2}[(\partial^2 k_1/\partial\omega_1^2)_{\omega_{10}} + (\partial^2 k_2/\partial\omega_2^2)_{\omega_{20}}] \quad (5)$$

The fluorescence power incident on the detector within a small bandwidth $d\omega_1$ is found by integrating Eq. (1) over ϕ. The result is

$$dP_1/d\omega_1 = (K\omega_1^4\omega_2 l P_3/G)\{S[(Gl\theta^2/2) - \beta] + S(\beta)\}, \quad (6)$$

where θ is the detector acceptance angle, $\beta = (b_0\omega + b_1\omega^2)l/2$, and

$$S(x) = \int_0^x \frac{\sin^2 u}{u^2}\,du. \quad (7)$$

When the second-order term $b_1\omega^2$ in Eq. (2) can be neglected (this is usually a good approximation far from degeneracy where $\omega_1 = \omega_2$), integration of Eq. (6) over all ω_1 gives the total fluorescence power as[12]

$$P_1 = (K\omega_1^4\omega_2 l P_3/|b_0|)\pi\theta^2 \quad (8)$$

The total power varies as θ^2 and increases near degeneracy since b_0 goes to zero.

The fluorescence bandwidth for a given θ and $d\omega_1$ is found from the full width at half-maximum (FWHM) of Eq. (6) plotted as a function of ω_1. An approximate result can be found, however, by considering the FWHM of the $\mathrm{sinc}^2(\Delta kl/2)$ function in Eq. (1). The first-order result is

$$\Delta\omega_1 = (1.77\pi/l|b_0|) + (G\theta^2/|b_0|). \quad (9)$$

It can be seen from Eq. (9) that the bandwidth is constant for small angles but varies as θ^2 for large angles. Like the total power, the bandwidth varies as $1/|b_0|$ and thus increases near degeneracy. The approximate power per unit bandwidth away from degeneracy is found by dividing Eq. (8) by Eq. (9):

$$P_1/\Delta\omega_1 = (\pi K l P_3/G)\{\theta^2/[(1.77\pi/Gl) + \theta^2]\}. \quad (10)$$

Note that the power per unit bandwidth approaches a constant value for large acceptance angles.

B. Experiment

We report here the first measurements of parametric fluorescence at wavelengths longer than 1 μ. The experimental arrangement used for our measurements is shown in Fig. 1. The $LiNbO_3$ nonlinear crystal was cut with a phase-matching angle of 49° and was antireflection coated so it could be placed inside the 1.064-μ Nd:YAG laser. Both laser mirrors were highly reflecting at 1.06 μ, and the one nearest the $LiNbO_3$ crystal was highly transmitting from 1.4 μ to 2.5 μ. In our experiments, the laser were operated cw in order to avoid damage to the crystal AR coatings.

Putting the nonlinear crystal inside the laser cavity provided a 25-fold increase in pump power. In the measurements discussed below, a maximum signal-to-noise ratio of 20–30 was observed. The increase in pump power resulting from intracavity operation was thus crucial to the success of the experiments. We feel this technique should make parametric fluorescence measurements possible in other laser–nonlinear crystal systems that previously have been limited by low available pump powers and insensitive detectors.

The results of our experimental measurements around 1.63 μ are shown in Fig. 2. The detector acceptance angle was varied by changing an aperture located in the focal plane of the collecting lens f_1. A monochromator bandwidth of 20 Å was chosen as a compromise between resolution and an acceptable signal-to-noise ratio. The solid theoretical curves are computed using Eq. (6) and the index data of Hobden and Warner.[21] Because of the difficulty in obtaining an absolute calibration of the detection system at 1.63 μ in terms of the in-crystal fluorescence power, the experimental points are normalized to the theoretical peak for each value of θ.

The theoretical crystal temperature was chosen so that the peak of the $\theta = 0.4°$ curve occurred at the experimentally observed wavelength and differed from the experimental oven temperature by +3.3°C. The discrepancy was caused by two factors. First, the 40-W pump power inside the laser heated the $LiNbO_3$ crystal. Second, it is known[22-24] that in $LiNbO_3$ the phase-matching temperature for a given nonlinear process varies with crystal composition. Using the technique of Pearson *et al.*[5], we found the temperature shift caused by the difference in composition of our crystal from that of Hobden and Warner to be $T_{calc} - T_{expt} = -1.9$°C. Since a difference of +3.3°C was necessary to match the fluorescence

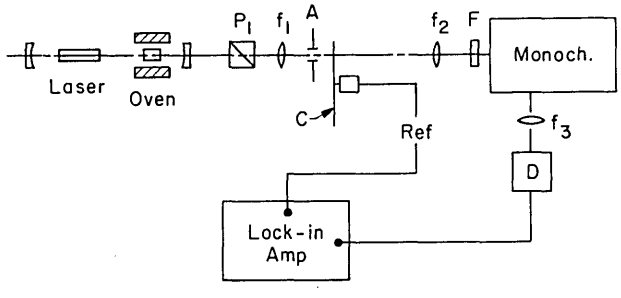

Fig. 1. Schematic of experimental arrangement for measuring ir narrow-bandwidth parametric fluorescence. Pump laser, cw Nd:YAG; P_1, polarizer; f_1,f_2, collecting and matching telescope; A, limiting aperture; C, chopper; F, visible and pump filters; f_3, short focal length lens; D, PbS photoconductive detector.

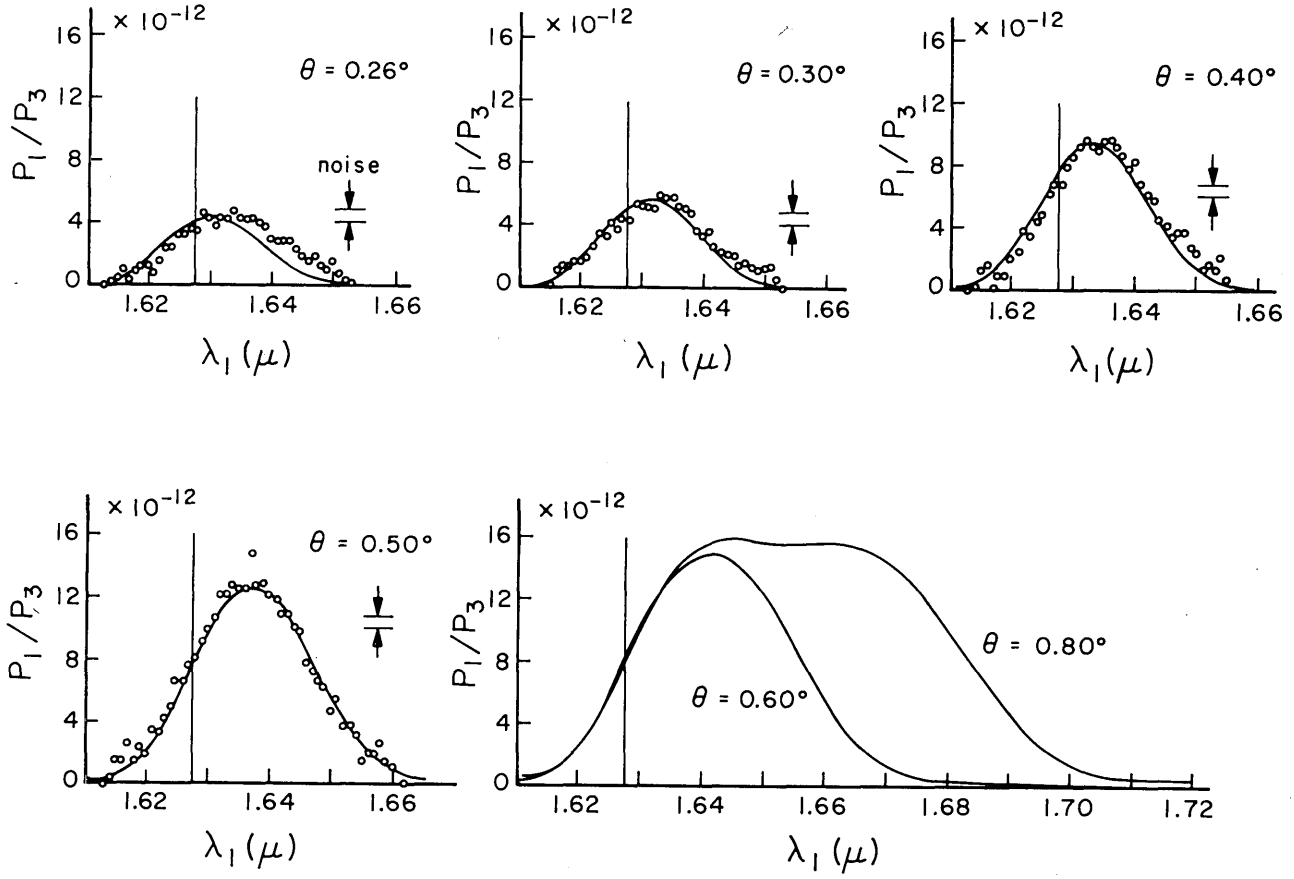

Fig. 2. Signal fluorescence power as a function of wavelength for various detector acceptance angles. The solid curves are theoretical with the temperature chosen to align the peak of the $\theta = 0.4°$ curve with the experimental peak (see text). The experimental data are normalized to the peak of each theoretical curve. The monochromator bandwidth is 20 Å and the experimental uncertainty is indicated in each figure. The vertical line at $\lambda_1 = 1.6278\ \mu$ is the collinear signal wavelength.

theory to experiment, the crystal was heated 5.2°C by the pump power.

Several of the qualitative features of the fluorescence theory are evident in Fig. 2. The full width at half-maximum bandwidth is nearly constant for small angles and the peak power (in our 20-Å bandwidth) becomes constant for large angles. For a 40-W pump, this limiting power corresponds to an in-crystal fluorescence power of 6.0×10^{-10} W. The approximate transmission of the optical system at 1.63 μ was 10% so that a maximum of 6×10^{-11} W of power was incident on the PbS detector.

The total fluorescence power as a function of θ^2 is shown in Fig. 3. The solid curve is found by integration of Eq. (6) over ω_1; the dashed line is found from Eq. (8). Since λ_1 is far from degeneracy, Eq. (8) accurately predicts the angular dependence of the total power. The experimental points in Fig. 3 are normalized to the theoretical value at $\theta^2 = 0.16$. The fluorescence bandwidth and peak power are shown in Figs. 4 and 5. The bandwidth values are taken directly from the experimental data, but the peak power data are normalized to the theoretical value at $\theta^2 = 0.28$. The agreement with theory is good within the experimental error. Note, however, that the approximate theoretical expressions, Eqs. (9) and (10), agree only qualitatively with the exact results found from Eq. (6).

The tuning curve of the 1.064-μ-pumped fluorescence is shown in Fig. 6. This is the tuning curve to be expected from a parametric oscillator using the same $LiNbO_3$ crystal and pump wavelength. To compare the experimental data with theory, two corrections must be made. First, the tuning data were taken with an acceptance angle of $\theta = 0.4°$. The peak of the monochromator scans will thus be shifted from the actual collinear wavelengths by an amount that depends on the crystal temperature. The experimental wavelengths are corrected for this shift using the index data of Hobden and Warner.[21] Second, the theoretical curve was shifted by +1.9°C (result of total power measurement; see Pearson *et al.*[5]), and the heating of the crystal was accounted for by increasing the oven readings by 5.2°C to find the actual crystal temperature. With these corrections, the solid theoretical curve in Fig. 6 agrees nicely with the experimental data.

Finally, the theoretical minimum bandwidth calculated from Eq. (9) with $\theta = 0$ is shown in Fig. 7 along with several experimental points. This is the

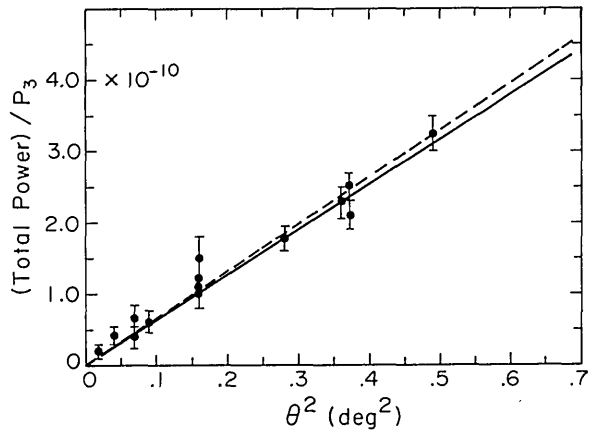

Fig. 3. Total signal power vs detector acceptance angle. The solid line is the theoretical in-crystal fluorescence power per unit pump power calculated using Eq. (6). The dashed line is found using the approximate expression, Eq. (8). The experimental data are normalized to the solid theoretical curve at $\theta^2 = 0.16$ deg^2.

bandwidth to be expected from a nonsteady-state parametric oscillator when the pump power is not strongly depleted. The experimental values were found by measuring the bandwidth with $\theta = 0.4°$ and correcting the results by a temperature-dependent factor to give the bandwidth for $\theta = 0$. The data have also been corrected for crystal heating and the theoretical curve shifted by +1.9°C as explained above.

III. 1.064-μ-Pumped Parametric Oscillation

In order to evaluate the usefulness of parametric fluorescence in predicting the properties of an OPO, two doubly resonant, 1.064-μ-pumped parametric oscillators were constructed. One oscillator operated near degeneracy ($\lambda_1 \simeq \lambda_2 \simeq 2.1\ \mu$), and the other was nondegenerate ($\lambda_1 \simeq 1.6\ \mu$, $\lambda_2 \simeq 3.2\ \mu$). The oscillators were operated internal to the Nd:YAG laser cavity and the laser was Q-switched at 400 Hz by a rotating mirror. The highly reflecting OPO mirrors were coated directly on the plane-parallel surfaces of the 5.5-mm $LiNbO_3$ crystals. A similar OPO design has been reported by Ammann *et al.*[2] A photograph of the Nd:YAG laser and OPO crystal oven is shown in Fig. 8.

This particular OPO laser design is particularly appealing because of its simplicity and compactness and because the number of components inserted into the laser is minimized. The OPO resonator is also automatically aligned. The internal OPO configuration allows maximum utilization of the available laser energy since the output coupling is provided by the OPO. Theoretically, 100% conversion of the available 1.064-μ average power to the OPO frequencies is possible,[25] and such operation has recently been observed by Ammann.[26]

The oscillator thresholds were found by turning down the laser drive power and measuring the polarized average 1.064-μ power when the OPO would barely flash. The laser duty cycle and mirror transmission at 1.064 μ then gave

$$P_{\text{thresh.}}\ (\text{one-way power}) = \begin{cases} 700 \pm 100\ \text{W}, & \lambda_1 \simeq 2\ \mu \\ 450 \pm 100\ \text{W}, & \lambda_1 \simeq 1.6\ \mu. \end{cases} \quad (11)$$

With an estimated one-way loss at both OPO frequencies of 2.5%, the computed threshold[27] for both oscillators was ≃300 W. The agreement is reasonable considering the approximate nature of the loss estimate (mainly mirror scatter) and the uncertainties in the experimental measurement.

A maximum average power of 6 mW at one frequency was observed from both the 1.6-μ and 2.1-μ oscillators. The average power varied by as much as a factor of 3 over the tuning range of each OPO. The observed pulse width was 25 nsec so that 6 mW corresponds to 600 W of peak power. The peak powers may be higher since the observed pulse width was nearly equal to the detection system response time.

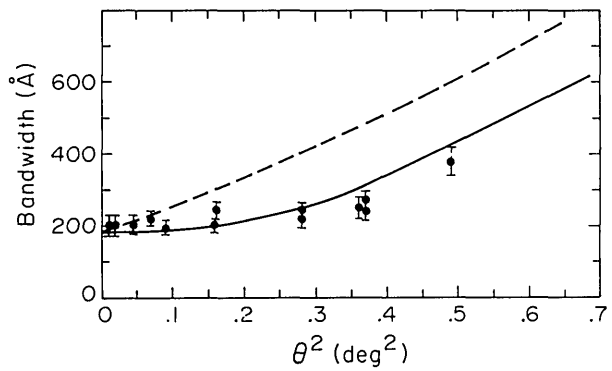

Fig. 4. Signal fluorescence bandwidth as a function of detector acceptance angle. The solid line is the exact theoretical bandwidth; the dashed curve is found from Eq. (9).

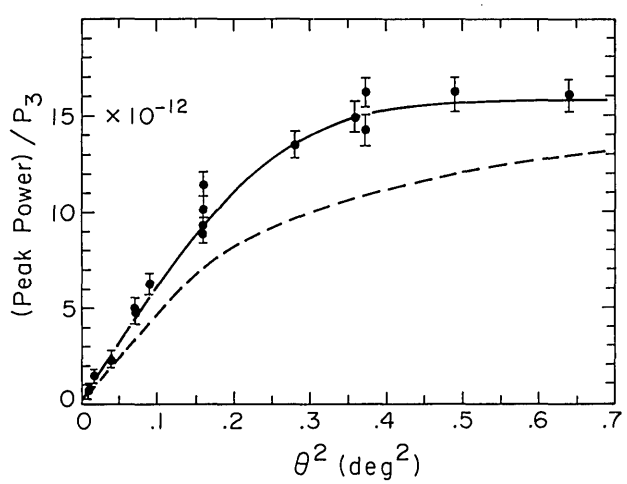

Fig. 5. Peak fluorescence power in a 20-Å bandwidth as a function of detector acceptance angle. The ordinate axis is the theoretical in-crystal fluorescence power per unit pump power. The experimental data are normalized to the theoretical curve at $\theta^2 = 0.28$ deg^2. Solid curve, exact theory, Eq. (6); dashed curve, approximate theory, Eq. (10).

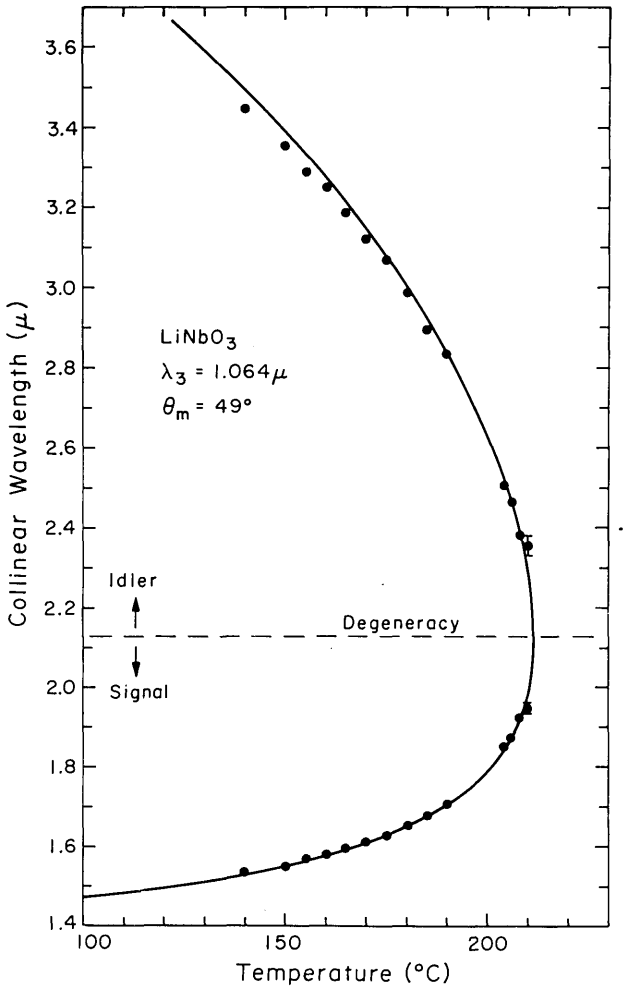

Fig. 6. Temperature tuning curve for 1.064-μ-pumped parametric fluorescence in $LiNbO_3$. The solid theoretical curve has been shifted by +1.9°C and the experimental data points are corrected for finite detector acceptance angle and crystal heating (see text).

With the OPO in the laser but below any oscillation temperature, the maximum polarized laser output power was 60 mW average and 1200 W peak (400-Hz, 130-nsec pulse). In terms of this available 1.06-μ power, both oscillators had a maximum average pump power conversion efficiency at *each* frequency of only 10%, but the peak power conversion efficiency was 50%. These efficiencies take into account only the power out one end of the OPO. Since an equal amount of power exits from the other end of the oscillator, the *overall* efficiencies are twice the above numbers. These efficiencies are comparable with those reported for many pulsed external OPO systems[11,28] but because of the high mirror reflectivities are still far short of the 100% average power efficiency observed by Ammann.[26]

For spectroscopic applications, the bandwidth and frequency stability of an OPO are important parameters. Both of these quantities will be adversely affected by mechanical and thermal instabilities, by pump frequency instabilities, and by the degree to which steady-state operation is achieved. In the oscillators reported here, mechanical instability of the OPO is not an important factor since the mirrors are coated directly on the nonlinear crystal and carefull oven design minimized the effects of temperature variations. The pump laser stability and the degree of steady-state operation were thus the limiting factors.

The tuning ranges and FWHM power spectral bandwidths are shown in Fig. 9 for both oscillators. The idler tuning range corresponding to the OPO of Fig. 9(b) is roughly 2.90 μ to 3.55 μ. The oscillator tuning characteristics were almost identical to the fluorescence tuning shown in Fig. 6. The observed bandwidths were only 10% of the fluorescence bandwidth, in contrast to a much closer agreement reported previously,[29] so the solid curves in Fig. 9 are normalized to the experimental data at the single point indicated by the large circle. The agreement of the experimental data with theory in Fig. 9 is only qualitative (larger bandwidth near degeneracy), and there is a large amount of scatter in the experimental data.

Although the observed bandwidth varied significantly from one operating point to another, the oscillator operation was quite stable and reproducible. The multicluster frequency instability usually associated with a doubly resonant OPO[6,30] was rarely observed. The center operating frequency was reproducible to within one or two multiples of the bandwidth over many system on–off cycles if the op-

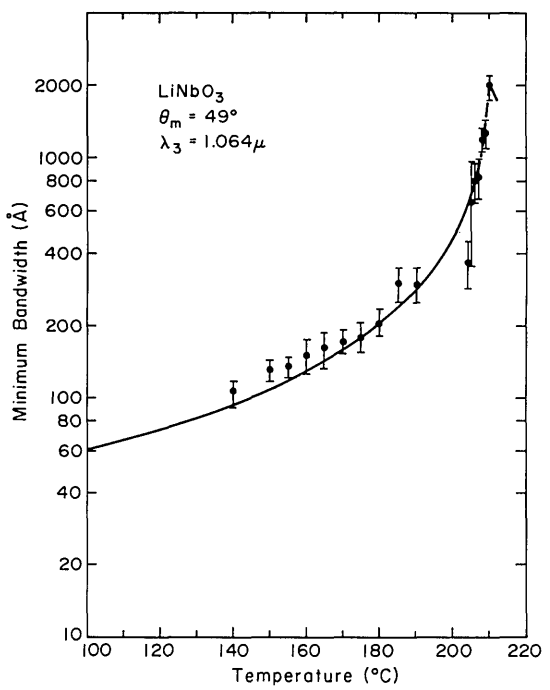

Fig. 7. Minimum bandwidth (collinear bandwidth) as a function of temperature in $LiNbO_3$. The pump wavelength is 1.064 μ, and the phase matching angle is 49°. The data have been corrected for finite detector acceptance angle and crystal heating and the theoretical curve is shifted by +1.9°C.

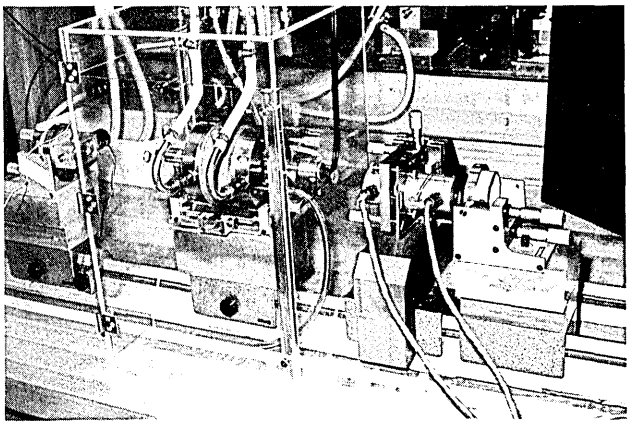

Fig. 8. Photograph of experimental setup showing Nd:YAG laser and temperature-controlled oven containing parametric oscillator crystal. Rotating mirror Q-switch is on the left.

tical alignment was not disturbed. The fact that the OPO bandwidths were smaller than the fluorescence bandwidths can be attributed to near-steady-state operation and to the cavity-dumping behavior of an internal OPO.[16] Both mechanisms can prevent lower-gain OPO frequencies from reaching significant oscillation levels.

Typical monochromator scans for two oscillators are shown in Fig. 10. The observed structure corresponds exactly to the longitudinal mode spacing of the OPO resonators and, to our knowledge, is the first reported observation of such distinct mode structure in an OPO. This type of spectrum was observed in the output of one pair of oscillators at all output powers and at all oscillation frequencies but was much less apparent in the output of two other pairs of oscillators that were pumped by a higher power laser. The precise reason for the appearance of the longitudinal mode structure in only one of the three pairs of oscillators is not understood, but it is suspected that the lower power laser plus OPO had a single-frequency pump, while the other laser–OPO combinations had a multifrequency pump. It is straightforward to show that a multifrequency pump would tend to wash out any OPO mode structure.[25]

The OPO transverse mode structure was studied at 1.6 μ using an image converter. Because of the flat–flat OPO resonator configuration, the oscillator transverse mode usually followed that of the pump laser, predominately TEM_{00}. Occasionally higher order modes were observed, and if the OPO mirrors became sufficiently damaged, the mode was very fragmented, bearing no relationship to the laser mode.

We have also observed the unique multiple-pulsing behavior of an internal OPO first discussed and observed by Falk *et al.*[16] At low drive levels, only a single OPO pulse is observed, as shown for our 1.6-μ oscillator in Fig. 11(a) along with an oscilloscope trace of the depleted pump pulse. Although the undepleted pump pulse width is 100–130 nsec, the OPO pulse width is only 20–25 nsec long [this is very near the resolution of our detection system (20 nsec); much shorter pulses can be expected[16]] and its peak occurs roughly near the peak of the undepleted pump pulse.

As the laser drive is increased, a second OPO pulse, and then a third appear as shown in Figs. 11(b) and 11(c). Note the stretching of the depleted pump pulse from 130 nsec (no oscillation) to over 200 nsec as multiple-pulse operation sets in. Further pump pulse stretching is limited by the high-Q time of our rotating mirror Q-switch. The appearance of the multiple-pulsing behavior is evidence of efficient OPO operation; the OPO is pumped so hard that it can dump the laser and actually drive the 1.06-μ field to zero.[16] Total average powers as high as 20 mW have been observed in the oscillators reported here, and higher powers would be expected with higher transmission OPO mirrors.

IV. Summary

By placing the nonlinear crystal inside the pump laser resonator, we have been able to measure parametric fluorescence in the infrared for the first time. The observed fluorescence total power, peak power,

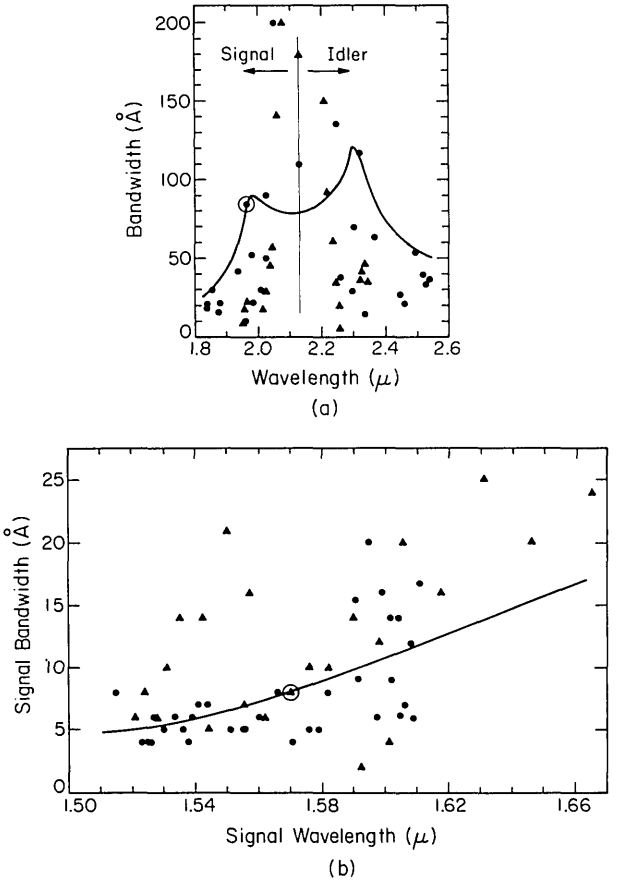

Fig. 9. Parametric oscillator full width at half-maximum spectral bandwidth for (a) 2.1-μ oscillator, and (b) 1.6-μ oscillator. The different symbols are for two different sets of mirror coatings. The solid curves are theoretical normalized to the experimental data at the circled points.

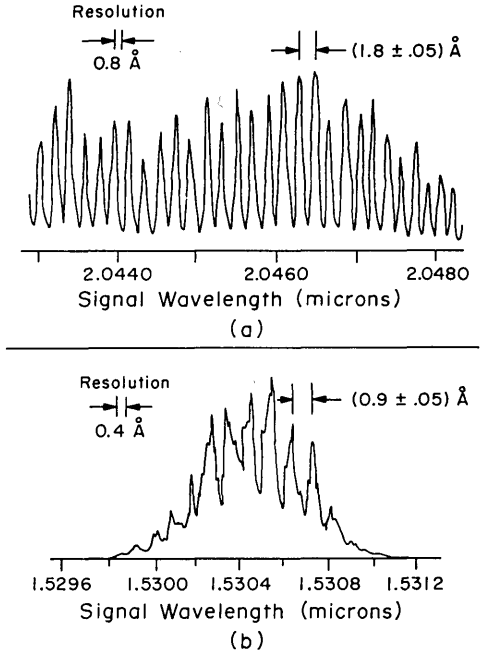

Fig. 10. Typical monochromator scans for oscillators pumped by lower power laser. (a) 2.1-μ oscillator. (b) 1.6-μ oscillator. The observed structure corresponds exactly to the longitudinal mode spacing of each oscillator.

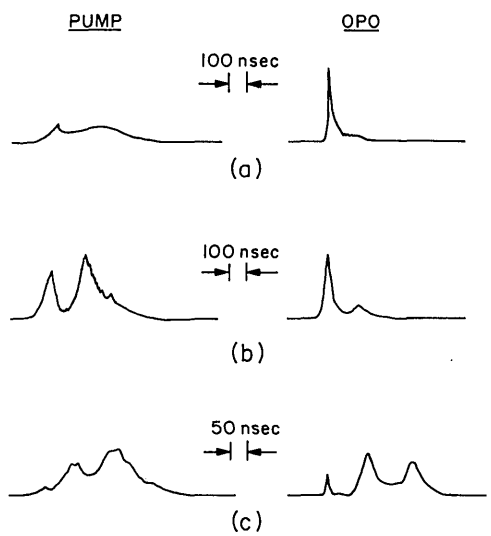

Fig. 11. Experimentally observed pulse shapes for the 1.6-μ oscillator for various pump laser drive levels. (a) Low drive level giving a single OPO pulse but showing strong pump depletion. (b) Stronger pumping than in (a). (c) Stronger pumping than in (b). The vertical scales in all the figures are arbitrary.

and bandwidth agree well with the plane-wave theory of Byer and Harris.[12] The techniques reported here should be applicable to other ir-pumped OPO systems where fluorescence measurements are desired but have been prevented by pump power limitations.

We have also reported the operating characteristics of two 1.064-μ-pumped pulsed, $LiNbO_3$ parametric oscillators. The two oscillators were doubly resonant, operated internal to the pump laser resonator, and provided tuning over most of the wavelength range from 1.51 μ to 3.55 μ. The oscillators were multifrequency but had bandwidths (1.7–45 cm^{-1}) an order of magnitude smaller than expected from the fluorescence measurements. The smaller bandwidths were attributed to near-steady-state operation and the cavity-dumping properties of an internal, pulsed parametric oscillator. Distinct longitudinal mode structure in an OPO was reported for the first time. Reasonable average powers (6 mW) and conversion efficiencies (10%) and good peak powers (600 W) and efficiencies (50%) were observed.

This work was supported by a grant from the General Dynamics Corporation, Pomona, California. Uri Ganiel was on leave from the Weizmann Institute of Science, and James Pearson was a Fannie and John Hertz Doctoral Fellow and is now at Hughes Research Laboratories.

References

1. E. O. Ammann, M. K. Oshman, J. D. Foster, and J. M. Yarborough, Appl. Phys. Lett. **15,** 131 (1969).
2. E. O. Ammann, J. M. - Yarborough, M. K. Oshman, and P. C. Montgomery, Appl. Phys. Lett. **16,** 309 (1970).
3. E. O. Ammann and J. M. Yarborough, Appl. Phys. Lett. **17,** 233 (1970).
4. D. C. Hanna, B. Luther-Davies, H. N. Rutt, and R. C. Smith, Appl. Phys. Lett. **20,** 34 (1972).
5. J. E. Pearson, U. Ganiel,and A. Yariv, IEEE J. Quantum Electron. **QE-8,** 383 (1972).
6. J. A. Giordmaine and R. C. Miller, Phys. Rev. **14,** 973 (1965).
7. R. G. Smith, J. E. Geusic, H. J. Levinstein, J. J. Rubin, S. Singh, and L. G. Van Uitert, Appl. Phys. Lett. **12,** 308 (1968).
8. J. E. Bjorkholm, Appl. Phys. Lett. **13,** 53 (1968).
9. J. Falk and J. E. Murray, Appl. Phys. Lett. **14,** 245 (1969).
10. L. S. Goldberg, Appl. Phys. Lett. **17,** 489 (1971).
11. R. W. Wallace, Appl. Phys. Lett. **17,** 497 (1971).
12. R. L. Byer and S. E. Harris, Phys. Rev. **168,** 1064 (1968).
13. S. E. Harris, M. K. Oshman, and R. L. Byer, Phys. Rev. Lett. **18,** 732 (1967).
14. C. Laurence and F. Tittel, Opto-Electron. **3,** 1 (1971).
15. A. Hordvik, H. R. Schlossberg, and C. M. Stickley, Appl. Phys. Lett. **18,** 448 (1971).
16. J. Falk. J. M. Yarborough, and E. O. Ammann, IEEE J. Quantum Electron. **QE-7,** 359 (1971).
17. W. H. Louisell, A. Yariv, and A. E. Siegman, Phys. Rev. **124,** 1646 (1961).
18. T. G. Giallorenzi and C. L. Tang, Phys. Rev. **166,** 225 (1968).
19. D. A.Kleinman, Phys. Rev. **174,** 1027 (1068).
20. D. Magde and H. Mahr, Phys. Rev. Lett. **18,** 905 (1967).
21. M. V. Hobden and J. Warner, Phys. Lett. **22,** 243 (1966).
22. J. E. Midwinter, J. Appl. Phys. **39,** 3033 (1068).
23. J. G. Bergman, A. Ashkin, A. A. Ballman, J. M. Dziedzic, H. J. Levinstein, and R. G. Smith, Appl. Phys. Lett. **12,** 92 (1968).
24. R. L. Byer, J. F. Young, and R. S. Feigelson, J. Appl. Phys. 41 2320 (1970).
25. J. E. Pearson, PhD Thesis, California Institute of Technology (1972).
26. E. O. Ammann, Rep. AFAL-TR-72-13, GTE Sylvania, Inc., Mountain View, Calif. (Jan. 1972).
27. G. D. Boyd and D. A. Kleinman, J. Appl. Phys. **39,** 3597 (1968).
28. L. B. Kreuzer, Appl. Phys. Lett. **13,** 57 (1968).
29. R. L. Byer, PhD Thesis, Stanford University (1968).
30. J. Falk, IEEE J. Quantum Electron. **QE-7,** 230 (1971).